Available online at www.sciencedirect.com
SCIENCE DIRECT®
International Journal of Multiphase Flow 31 (2005) 302–317
International Journal of Multiphase Flow
www.elsevier.com/locate/ijmulflow

Pulsating, buoyant bubbles close to a rigid boundary and near the null final Kelvin impulse state

E.A. Brujan [a,*], A. Pearson [b], J.R. Blake [b]

[a] Department of Hydraulics, University Polytechnica, Spl. Independentei 313, 060042 Bucharest, Romania
[b] School of Mathematics and Statistics, The University of Birmingham, Edgbaston, Birmingham B15 2TT, UK

Received 2 January 2004; received in revised form 23 November 2004

Abstract

This theoretical and computational study provides insight into the behaviour of large bubbles generated by underwater explosions near the seabed and airguns close to supporting structures when at least two opposing forces influence bubble behaviour. A null final Kelvin impulse occurs when these forces are in balance over a pulsation. Likewise for smaller bubbles such as occur in levitation phenomena for bubbles in a sound field, an 'equilibrium' bubble position is achieved. In both cases, energy dissipation mechanisms near minimum volume are important in determining subsequent bubble behaviour. Two cases typify the jetting behaviour near the null final Kelvin impulse state: (i) formation of an inward-flowing circular radial jet leading to bubble splitting, and (ii) formation of two opposite high-speed axial jets directed towards the bubble centre. The complex behaviour is attributed to a slight difference between the strength of the opposing forces acting on the bubble during growth and collapse. The present results indicate that the jetting behaviour in the neighbourhood of the neutral bubble collapse can be adequately described by the Kelvin impulse itself, but evaluated during the collapse phase of the bubble. Its direction determines the position of the radial jet in the initial phase of the collapse while its magnitude indicates the degree of asymmetry of the bubble-split and the intensity of the radial jet. Both factors are essential in estimating the final fate of the bubble at the neutral collapse state. Away from this null-state, the final Kelvin impulse is a valuable tool in predicting the migratory characteristics of the bubble and the direction of the axial jet developed during bubble collapse.

* Corresponding author.
E-mail address: eabrujan@yahoo.com (E.A. Brujan).

0301-9322/$ - see front matter © 2004 Elsevier Ltd. All rights reserved.
doi:10.1016/j.ijmultiphaseflow.2004.11.006

Keywords: Buoyant bubble; Kelvin impulse; Jet formation

1. Introduction

Pulsating buoyant bubbles acted upon by opposing forces have particular relevance to the motion of underwater explosion bubbles and airgun generated bubbles (diameter 0.5–10 m) near the seabed, the sea surface or structures. In some cases the forces acting on a bubble over a pulsation may be in near equilibrium. This aspect is best measured by a quantity known as the Kelvin impulse, in effect the time integral of the forces acting, which will have a value near zero at the end of a pulsation for equilibrium cases. This is referred to as the 'null final Kelvin impulse state'. This near equilibrium state is also relevant to levitated acoustic bubbles as occurs in single bubble sonoluminescence or sonochemistry. Additionally, energy loss and dissipation mechanisms near minimum volume are not well understood leading to poor subsequent predictions of bubble rebound behaviour. Understanding the likely bubble topology, the bubble surface velocities, especially any jetting behaviour that might occur, and the pressure field surrounding a bubble will lead to an enhanced understanding of the likely energy loss and dissipation mechanisms such as jetting, acoustic radiation, viscous forces and turbulence as well as the partitioning of energy into potential and kinetic energy at different stages of the bubble period.

Since the classic work of Rayleigh (1917), the collapse of a cavity has been treated with various degrees of sophistication. Rayleigh analysed the collapse of an empty spherical bubble in a liquid of infinite extent under an excess pressure. Other works have included the effects of surface tension, viscosity and compressibility (see, for example, Prosperetti and Lezzi, 1986 and the references therein). Kornfeld and Suvorov (1944) were the first to suggest that bubbles might collapse asymmetrically and produced a jet. The asymmetry of the collapse is a result of a pressure gradient. In the case when this pressure gradient is provided by a rigid boundary, often a jet forms which is directed onto the surface (Plesset and Chapman, 1971). The most significant parameter affecting the dynamical properties of the jet is the non-dimensional stand-off, defined as the distance of the initial location of the bubble from the boundary scaled by the maximum bubble radius, which is denoted by γ (Blake et al., 1986; Vogel et al., 1989).

In addition to the pressure gradient generated by the rigid boundary, a large pulsating, buoyant bubble is subjected to a second pressure gradient induced by the gravitational field. Depending on the direction and the relative strength of the pressure gradients a large variety of the jetting behaviour was identified which includes the formation of an inward-flowing circular radial jet (hereafter called a radial jet) and axial jets directed towards and away from the boundary. Classic examples are given in the papers by Blake et al. (1986) and Best and Kucera (1992). The evidence of the numerical computations presented in these papers also indicates that the direction of the jet and the direction of the Kelvin impulse at the end of the collapse (final Kelvin impulse state) are closely correlated. A less understood aspect of the bubble dynamics is the jetting behaviour near the null final Kelvin impulse state. This case is particularly interesting because the opposing forces acting on the bubble motion, namely the downward directed pressure-gradient force directed towards the boundary and the upward buoyancy force, lead to a near zero Kelvin impulse at the end of bubble collapse.

In this paper, the dynamics of a pulsating, buoyant bubble situated above a rigid boundary near the null final Kelvin impulse state is investigated numerically using a boundary integral method. The results of the numerical computations provide the bubble profiles and the pressure contours in the liquid surrounding the bubble. We found a complex jetting behaviour which depends strongly on the initial location of the bubble from the boundary. At small γ-values, an asymmetric radial jet is formed leading to bubble splitting. At larger γ-values, two axial jets directed towards the bubble centre are developed during the collapse phase of the bubble as a consequence of a more symmetric but weaker radial jet in the initial phase of bubble collapse. Each jet is further accelerated during the final stage of the bubble collapse by a high pressure region that develops when the bubble wall is already indented. The complex jetting behaviour is attributed to a difference between the strength of the opposing forces during the collapse phase of the bubble.

We believe that the present results are interesting in two complementary ways. First, they reveal the complex jetting behaviour of a bubble situated in two opposing pressure gradients in the neighbourhood of the null final Kelvin impulse state. Secondly, the results give insight into the energetics of the final stages of a violently collapsing bubble that will be invaluable in understanding pressures, stresses and energy dissipation mechanisms which may have bearing on the behaviour of bubbles, materials and molecules in a range of medical and industrial applications (e.g. shock wave lithotripsy, laser surgery, gene expression, therapeutic ultrasound and sonochemistry).

The fluid mechanics of energetic, pulsating, buoyant bubbles are dominated by inertial effects because of the high velocities and short time scales leading to very high Reynolds number flows. Therefore we model the fluid mechanics by an inviscid and incompressible fluid where the motion is irrotational. Well established boundary integral techniques (e.g. Best and Kucera, 1992; Pearson et al., 2004) accurately model the highly non-linear and non-spherical bubble behaviour extremely accurately. Pressures are typically large so that surface tension effects may be neglected. However, buoyancy forces are important in this case. We define a buoyancy parameter δ as follows:

$$\delta = \left(\frac{\rho g R_{\mathrm{m}}}{\Delta p}\right)^{1/2} \tag{1}$$

with ρ the density of the fluid, g gravitational acceleration, R_{m} maximum bubble radius, and $\Delta p = p_{\infty} - p_{\mathrm{v}}$ the pressure scale obtained from the difference between the ambient pressure at the point of bubble generation and the vapour pressure. Physically, δ corresponds to the ratio of the velocity of the buoyant motion of the bubble, $(gR_{\mathrm{m}})^{1/2}$, to the characteristic velocity of bubble growth or collapse $(\Delta p/\rho)^{1/2}$. In the calculations that follow, this latter velocity will be used to scale velocities, R_{m} to scale length and Δp pressures.

The pressure inside the cavity is assumed to be uniform and consists of a constant vapour pressure and a volume-dependent non-condensible gas pressure. A simple adiabatic model is used for the variation of cavity pressure, p_{c}, giving

$$p_{\mathrm{c}} = p_{\mathrm{v}} + p_0(V_0/V)^{\kappa}, \tag{2}$$

where p_0 is the initial pressure of the non-condensable gas inside the bubble (corresponding to a bubble volume V_0) and κ is the ratio of specific heats. The assumption of a uniform gas pressure is likely to be inaccurate over the last few percent of the collapse time but one would not expect this circumstance to induce order-of-magnitude errors in the results.

Initial conditions are dependent on the particular application. For example, direct modelling of the temporal evolution and spatial distribution of the energy deposition during detonation is complicated, and details depends strongly on the type and geometry of the explosive charges (Cole, 1948). We therefore neglect the details of the detonation process and assume that the bubble originates from a small spherical cavity of radius R_0, wall velocity v_0, and internal pressure p_0 which subsequently grows to many times its initial volume. The constants in the above equations are: density of water $\rho = 998\ \mathrm{kg/m^3}$, polytropic exponent of air $\kappa = 1.4$, vapour pressure $p_v = 2.35$ kPa, and static ambient pressure $p_\infty = 100$ kPa. The initial radius is chosen such that the maximum dimensionless radius to which the bubble would expand in an infinite fluid is equal to one and this value is obtained from an energy balance equation. The other two values adopted as initial conditions are $\alpha = p_0/(p_\infty - p_v) = 100$ and $v_0 = 10$. It should be noted here that different values of the initial pressure and radial velocity show the same gross structure of bubble dynamics at null final Kelvin impulse state, with just shifted values in the γ–δ parameter space. This has been confirmed by some trial calculations with v_0 in the range 1–100 and α up to 1000.

2. Kelvin impulse

The concept of the Kelvin impulse, which was applied to bubble dynamics by Benjamin and Ellis (1966), provides a useful theoretical framework for interpreting the behaviour of a bubble near boundaries. The Kelvin impulse can be interpreted as a linear impulse of the bubble if one attributes a virtual mass to the bubble which corresponds to the liquid mass moving around the cavity. Since axial jets are associated with bubble migration in the direction of the jet, it was suggested that their occurrence and direction can be predicted by analysing the Kelvin impulse at the end of the bubble collapse (Blake et al., 1986, 1987, 1997; Best and Kucera, 1992; Best and Blake, 1994).

The Kelvin impulse of a cavity (scaled by $R_m^3(\rho\Delta p)^{1/2}$) is defined as

$$\boldsymbol{I} = \int_{S_b} \phi \boldsymbol{n}\, \mathrm{d}S, \tag{3}$$

where S_b is the surface of the bubble. The sense of the normal vector to the surface, $\boldsymbol{n}$, is taken to be positive into the bubble interior. The rate of change of the Kelvin impulse is given by (Blake and Cerone, 1982)

$$\frac{\mathrm{d}\boldsymbol{I}}{\mathrm{d}t} = \boldsymbol{F}^{\Sigma} + \boldsymbol{F}^{g}, \tag{4}$$

with

$$\boldsymbol{F}^{\Sigma} = -\int_{S_b} \left\{ \frac{1}{2}|\nabla\phi|^2 \boldsymbol{n} - \frac{\partial\phi}{\partial n}\nabla\phi \right\} \mathrm{d}S, \tag{5}$$

and

$$\boldsymbol{F}^{g} = \delta^2 V \boldsymbol{e}_z, \tag{6}$$

$\boldsymbol{e}_z$ being a unit vector in the positive z-direction. $\boldsymbol{F}^g$ is the buoyancy force and $\boldsymbol{F}^\Sigma$ is the pressure-gradient Bjerknes force exerted by the boundary. These expressions can also be derived by using the fact that the hydrodynamic force, $\boldsymbol{F}_\mathrm{h}$, on the bubble is zero, where

$$\boldsymbol{F}_\mathrm{h} = -\frac{\mathrm{d}\boldsymbol{I}}{\mathrm{d}t} - \int_{S_\mathrm{b}} \left\{ \frac{1}{2}|\nabla\phi|^2 \boldsymbol{n} - \frac{\partial\phi}{\partial n}\nabla\phi \right\} \mathrm{d}S + \delta^2 V \boldsymbol{e}_z. \tag{7}$$

It is evident from (4) that the Kelvin impulse is a function of time, starting from zero at inception and changing sign during the lifetime of the bubble depending on the relative strength of the forces acting on the bubble motion. The interesting feature of (4) is the existence of a null final Kelvin impulse state defined by $\boldsymbol{I} = \int(\boldsymbol{F}^\Sigma + \boldsymbol{F}^g)\,\mathrm{d}t = 0$ at the end of the first bubble pulsation for appropriately related values of γ and δ with the exact nature of this relationship being determined later in this section. The choice of time at the end of the first pulsation is based on the (normal) observation that a bubble remains near spherical for much of its lifetime (~95%), only developing significant non-sphericity at the end of the pulsation where the additional contributions to the Kelvin impulse are small ($O(R)$). It is at this state that the strength of the competing pressure-gradient and buoyancy forces is equal and the centroid of the bubble maintains its initial position.

A comment on the calculation of the Kelvin impulse is appropriate here. When the bubble is initiated very close to the rigid boundary ($\gamma < 0.7$) the computations break down before the bubble reaches the minimum volume because the liquid layer between bubble and wall is extremely thin and, therefore, the final Kelvin impulse of the bubble cannot be accurately calculated. In this case, the null final Kelvin impulse state of the bubble is estimated by considering the centroid position in a very late stage of bubble collapse. With increasing initial distance between bubble and boundary, the computations better describe the final stages of bubble collapse and the calculated value of the final Kelvin impulse becomes more accurate.

Several relatively simple models can assist with defining the γ–δ parameter space of the Kelvin impulse for energetic, pulsating, buoyant bubbles. The simplest model represents the bubble as a time-dependent source at a fixed stand-off distance h above a rigid boundary (Blake et al., 1986; Blake, 1988). The 'final' Kelvin impulse of the spherical model bubble at the end of the first collapse $I_x(t_\mathrm{c})$ is

$$I_x(t_\mathrm{c}) = \frac{2\sqrt{6}\pi R_\mathrm{m}^5(\rho\Delta p)^{1/2}}{9h^2}[2\gamma^2\delta^2 B(11/6,1/2) - B(7/6,3/2)], \tag{8}$$

where $B(p,q)$ is a Beta function. The first term in (8) corresponds to the integrated buoyancy condition whereas the second term is associated with a pressure-gradient Bjerknes force directed towards the rigid boundary. For the null 'final' Kelvin impulse state this is set equal to zero to yield the following relationship between γ and δ

$$\gamma\delta = \left[\frac{B(7/6,3/2)}{B(11/6,1/2)}\right]^{1/2} \approx 0.442. \tag{9}$$

A slightly more sophisticated model was developed by Best (Best, 1991; Best and Blake, 1992) which allowed the spherical bubble to move in the vertical direction by adding a time-dependent dipole to the previous source as well as various image systems to maintain the sphericity of the bubble. To this we add a term to account for the presence of the adiabatic gas content. This leads

to the set of coupled ODE's for the motion of the bubble for the following dimensionless variables: radius R, bubble depth H and translational velocity U:

$$R\ddot{R}\left(1+\frac{R}{2H}\right)+\frac{3}{2}\dot{R}^2\left(1+\frac{2R}{3H}\right)-\frac{1}{4}U^2=\alpha\left(\frac{R_0}{R}\right)^{3\kappa}+\delta^2(H-\gamma)-1, \tag{10a}$$

$$\frac{\mathrm{d}}{\mathrm{d}t}(R^3U)=\frac{3}{4}\frac{R^4}{H^2}(3\dot{R}^2+R\ddot{R})+2\delta^2R^3, \tag{10b}$$

$$U=\frac{\mathrm{d}H}{\mathrm{d}t} \tag{10c}$$

subject to appropriate initial conditions discussed earlier

$$\begin{aligned} &R(0)=0.1383, \quad \dot{R}(0)=10,\\ &H(0)=\gamma, \quad U(0)=0. \end{aligned} \tag{10d}$$

This leads to an expression for the Kelvin impulse of

$$I=\frac{2}{3}\pi\left[R^3U-\frac{3}{4}\left(\frac{R}{H}\right)^2R^3\dot{R}\right]. \tag{11}$$

These equations may be integrated numerically to yield a graph for the zero Kelvin impulse state at the end of the first collapse similar to that obtained from (9) but shifted to the left (see Fig. 5 later).

3. Results

3.1. Kelvin impulse, bubble migration and jet formation

The purpose of the computed examples presented here is to provide a framework showing the range of possible behaviours when a bubble is subjected to two opposite pressure gradients, further developing the studies of previous authors (Blake et al., 1986; Best and Kucera, 1992).

Fig. 1 shows the relation between jet formation, centroid migration and final Kelvin impulse for a stand-off of $\gamma=1$. When the magnitude of the opposing forces is near equal, the final Kelvin impulse is close to zero and a symmetric radial jet is observed in a late collapse stage. A radial jet may also develop when the strength of the opposing forces are not equally strong, but it will be displaced slightly in response to these differences. For example, the radial jet is located at the bubble part closer to the boundary when the final Kelvin impulse is directed away from the boundary ($I(t_c)>0$), while if it is directed towards the boundary ($I(t_c)<0$) the radial jet will be located at the bubble part far from the boundary. Obviously, the larger the absolute value of the final Kelvin impulse, the more displaced is the position of the radial jet during bubble collapse. In the very late stages of the collapse, the radial jet leads to bubble splitting and the generation of two high-speed axial jets in opposite direction (see, for example, Blake et al., 1997). These bubble characteristics have been also observed for motion between parallel plates (Chahine, 1982), in an

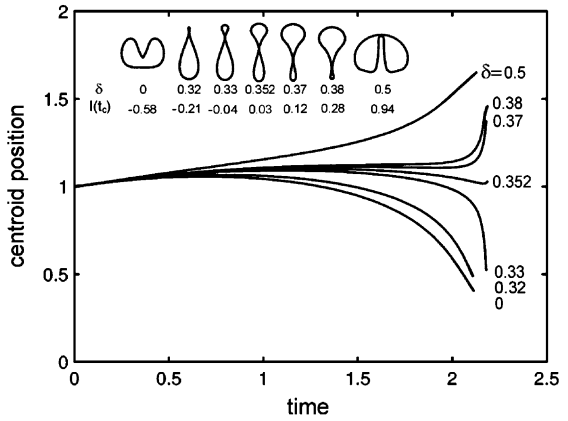

Fig. 1. Centroid position of a bubble situated above a rigid boundary for $\gamma = 1$ and different values of the buoyancy parameter. The computed bubble shape in the final collapse stage is also illustrated. The value of the Kelvin impulse at the end of the collapse is given below each bubble shape. The null final Kelvin impulse state of the bubble is considered to occur for $\delta = 0.352$, although the calculated value of the final Kelvin impulse is 0.03. It is at this δ-value that the centroid position in the very late collapse stage is close to the initial distance between bubble and boundary. Slightly larger or smaller values of δ result in bubble migration away-from and towards the boundary, respectively.

axisymmetric stagnation flow towards a rigid boundary (Robinson and Blake, 1994), and near an elastic boundary (Brujan et al., 2001a,b). In the limit, however, when one of the forces dominates, only one axial jet is formed and the bubble migrates in the direction of the dominant force. Later in the collapse phase the axial jet penetrates the opposite bubble wall and the bubble takes a toroidal shape (see, for example, Brujan et al., 2002, Pearson et al., 2004).

A very interesting phenomenon is observed for a stand-off of $\gamma = 2$ (Fig. 2). The transition from jet formation directed downwards to jet formation directed upwards, as the relative strengths of the buoyancy and pressure-gradient forces change, consists of two axial jets directed towards the

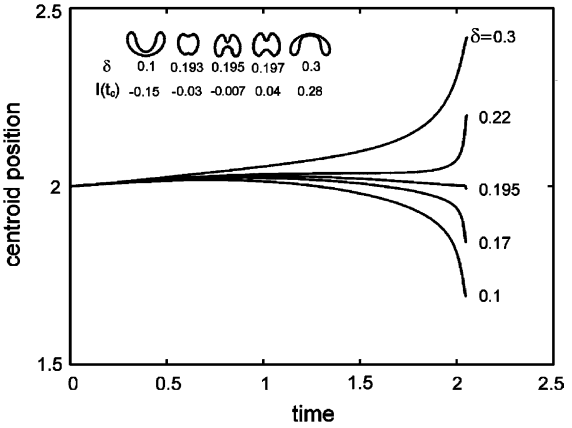

Fig. 2. Centroid position of a bubble situated above a rigid boundary for $\gamma = 2$ and different values of the buoyancy parameter. The computed bubble shape in the final collapse stage is also illustrated. The value of the Kelvin impulse at the end of the collapse is given below each bubble shape.

bubble centre. At the near null final Kelvin impulse state of the bubble the upper jet is faster and thinner than the lower one. At larger positive values of the final Kelvin impulse the lower jet becomes dominant, while the dominance of the upper jet is preserved at smaller negative values of the final Kelvin impulse. Similar results have been reported for the motion of a bubble situated in a rearward stagnation-point flow near a rigid boundary (Blake et al., 1986). We further note that, in both examples, the direction of the final Kelvin impulse coincides with the direction of bubble migration.

3.2. Bubble dynamics near the null final Kelvin impulse state

In this section we give representative examples of the dynamics of a pulsating, buoyant bubble close to a rigid boundary and near the null final Kelvin impulse state. Two typical cases are identified as the initial location of the bubble from the rigid boundary is increased: (i) formation of a radial jet leading to bubble splitting, and (ii) formation of two opposite axial jets directed towards the bubble centre. In the following, part (a) of each figure shows the calculated bubble shapes while part (b) shows the flow field in the liquid surrounding the bubble in a final stage of the collapse.

Fig. 3a illustrates the temporal development of the bubble shape when the values of the stand-off and buoyancy parameter are $\gamma = 1$ and $\delta = 0.352$. Although during the initial growth phase the bubble keeps its near spherical symmetry, at maximum volume it becomes flattened in a direction parallel to the boundary. Once the oblate shape of the bubble is formed ($t = 1.001$), it collapses from its sides leading to the production of a radial flow which is more pronounced around the surface of the bubble closer to the rigid boundary. Therefore, an ''egg-timer'' shape of the bubble develops in a later stage of the collapse (frames 5–7). An additional factor contributing to the formation of the ''egg-timer'' shape is the low pressure region between the collapsing cavity and the boundary which keeps the bubble close to the boundary. The maximum dimensionless velocity of the radial jet is 28 (approximately 280 m/s in absolute value) and is reached in the final stage of bubble collapse. At time $t = 2.183$, pinch-off is observed to occur and the bubble splits in two. Had the calculations been allowed to continue, two high-speed axial jets emanating from the high-curvature regions of closure would be formed, the lower of which would strike the boundary with an ultra high velocity (Blake et al., 1997). The pressure field at the conclusion of collapse is given in Fig. 3b. It can be seen that the jet is further accelerated during the late stages of the collapse by a ring-shaped region of high pressure with a magnitude of 90 (9 MPa in absolute value) surrounding the bubble that develops when the bubble walls are already indented.

When the bubble is initiated far from the boundary (Fig. 4a; $\gamma = 2$, $\delta = 0.195$), it retains much of its spherical symmetry at the maximum expansion. In this case the flow field is more symmetrical and the formation of a radial flow occurs around the bubble equator. The bubble acquires the form of a prolate spheroid during the initial collapse phase (frames 4 and 5). Subsequently, two axial liquid jets directed towards bubble centre develop at the bubble poles. The jet directed away from the boundary develops first as a result of a higher curvature of the bubble wall close to the boundary. We note that whereas the maximum velocity of the axial jet directed towards the boundary is 30 the corresponding value for the axial jet directed away from the boundary is about 18. The fluid speed upon collapse is so high that both jets penetrate the bubble sufficiently that the bubble does not rebound in connected form. The damage capability of the bubble is even smaller

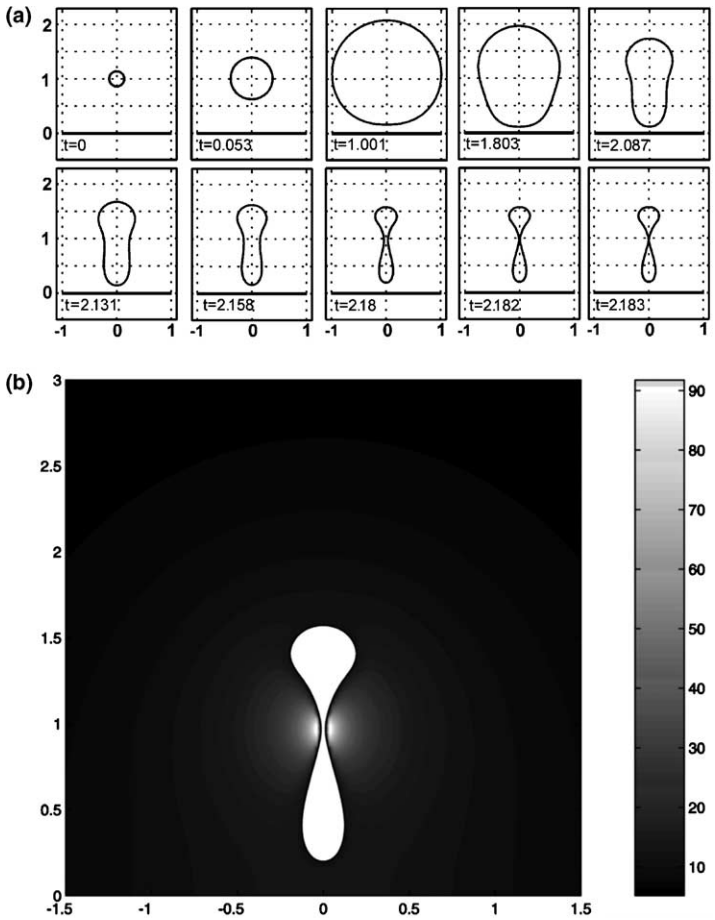

Fig. 3. Bubble dynamics at the null Kelvin impulse state for $\gamma = 1$ and $\delta = 0.352$. (a) Variation with time of the bubble shape. (b) Pressure contours in the liquid surrounding the bubble in the final stage of bubble collapse ($t = 2.182$).

in this case, on one hand, because the bubble is too far from the boundary at the end of the collapse and, on the other hand, the axial jets interfere with one another in the final collapse stage. The formation of two opposite axial jets was also observed experimentally during the collapse of cylindrical bubbles in a liquid of infinite extent (Godwin et al., 1999). In Fig. 4b, the pressure contours in the liquid surrounding the bubble are given for $t = 2.048$. It is clearly indicated that the presence of two local peak pressures located above and below the bubble is responsible for the acceleration of both jets during the very late stages of the collapse. The magnitude of the high pressure regions is about 500. The rigid boundary leads to a prolongation of the collapse time of the bubble and to a decrease of the maximum pressure in the liquid surrounding the bubble. For large γ-values, the collapse is almost spherical and the axial jets develop only at a very late stage of the collapse. The liquid moves almost radially towards the collapse centre, leading to a violent collapse with a strong compression of the bubble contents. For small γ-values, the radial flow is dominant while the upper and lower sides of the bubble are almost motionless (Fig. 3a,

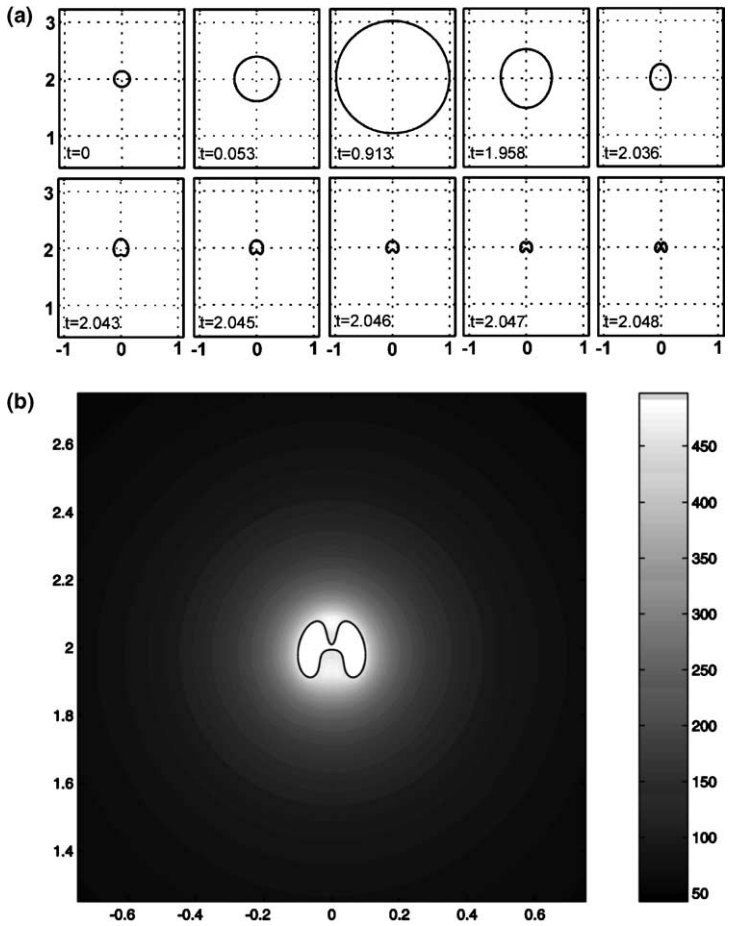

Fig. 4. Bubble dynamics at the null Kelvin impulse state for $\gamma = 2$ and $\delta = 0.195$. (a) Variation with time of the bubble shape. (b) Pressure contours in the liquid surrounding the bubble in the final stage of bubble collapse ($t = 2.048$).

frames 6–10). As kinetic energy is clearly associated with this motion, the bubble content becomes less compressed than in the case of large γ-values (compare the minimum bubble sizes for the cases illustrated in Figs. 3 and 4) so the pressure amplitude in the surrounding liquid is diminished.

3.3. Jetting behaviour as a function of γ and δ

Fig. 5 gives an overview of the jetting behaviour as a function of the normalized distance between bubble and boundary γ and the buoyancy parameter δ, thus identifying the regions of parameter space where the near equilibrium behaviour associated with a null Kelvin impulse may be found. The solid line denotes the null final Kelvin impulse state where the bubble centroid maintains its initial position at the end of the collapse (neutral bubble collapse). States described by points lying above the null final Kelvin impulse curve ($I(t_c) > 0$) correspond to bubble migration away from the boundary, while points lying below the null final Kelvin impulse curve

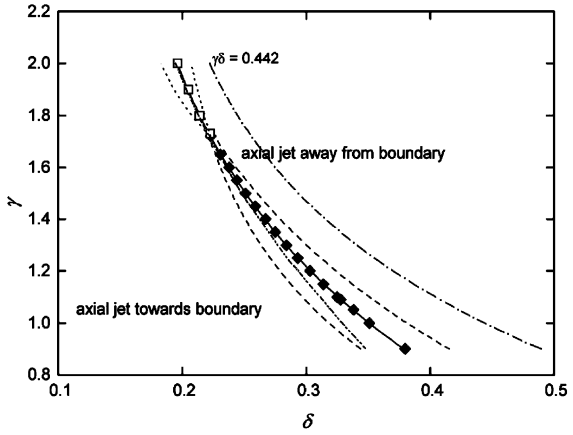

γ	δ (BIM)	δ (Eqs.15 and 16)
2	0.196	0.1944
1.9	0.205	0.2033
1.8	0.214	0.2129
1.73	0.2227	0.2185
1.72	0.223	0.2188
1.65	0.231	0.2291
1.6	0.238	0.2350
1.55	0.244	0.2411
1.5	0.251	0.2476
1.45	0.259	0.2543
1.4	0.267	0.2614
1.35	0.275	0.2688
1.3	0.284	0.2765
1.25	0.293	0.2845
1.2	0.303	0.2928
1.15	0.314	0.3015
1.1	0.325	0.3105
1.05	0.338	0.3197
1	0.351	0.3291
0.9	0.381	0.3482

Fig. 5. Jetting behaviour of a pulsating, buoyant bubble situated above a rigid boundary as a function of the stand-off γ and buoyancy parameter δ. The solid line denotes the null final Kelvin impulse state of the bubble. Filled symbols: radial jet leading to bubble splitting and open symbols: two opposite axial liquid jets developed during bubble collapse. The dashed line surrounds the region where an radial jet leading to bubble splitting is generated and the dotted line the region where two opposite axial jets directed towards the bubble centre are observed. For comparison, the analytical estimate of the null Kelvin impulse state using point source solutions (Blake, 1988) (dash and dot line) and the results obtained by using Eqs. (15) and (16) (dashed line with two dots) are also shown in the figure. The values of γ and δ at the null final Kelvin impulse state obtained using the boundary integral method (BIM) and Eqs. (15) and (16) are also shown.

($I(t_c) < 0$), correspond to bubble migration towards the boundary. The zones where only one axial jet develops during bubble collapse are separated by regions centred around the null final Kelvin impulse curve with a complex jetting behaviour. For small γ-values, a radial jet develops leading to bubble splitting and the formation of two axial jets directed towards and away from the boundary. The bubble achieves an oblate shape in the early collapse phase and collapses faster from the sides in a later stage. This leads to the formation of a strong radial jet which finally separates the upper and lower parts of the bubble and generates two axial jets flowing in opposite directions. For large γ-values, two opposite axial jets directed towards the bubble centre are formed in the final stage of the collapse. In this case, the magnitude of the opposite forces acting on the bubble motion is, however, too small to induce a pronounced flattening of the bubble into an oblate shape which would lead to the formation of a strong radial jet. For example, for $\gamma = 2$ and $\delta = 0.195$, the horizontal axis of the expanded bubble is only about 5% longer than the vertical axis (Fig. 4a, frame 3). Because of this small deviation from sphericity the liquid is preferentially drawn in from the sides only in a very late stage of the collapse and the bubble becomes elongated along the axis of symmetry. Also included in this figure are the results predicted by the spherical model of Best (1991) and the analytical estimate of the null final Kelvin impulse state as obtained by Blake (1988). For motion in the closest proximity to the rigid boundary the spherical model fails to give an adequate estimate of the final Kelvin impulse. However, as the point of inception moves away from the boundary the agreement improves substantially. It is evident that the simple analysis based on the Kelvin impulse at the end of the collapse does not portray the whole complexity of the jetting behaviour in the neighbourhood of the neutral collapse state of the bubble. It represents, however, a valuable tool in predicting the migratory characteristics of the bubble.

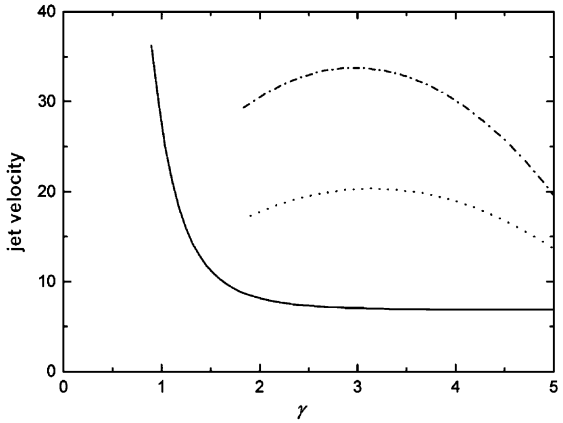

Fig. 6. Velocity of the radial jet (solid line) and axial jets directed towards the bubble centre (upper jet: dash and dot line, lower jet: dotted line) developed during bubble collapse at the null Kelvin impulse state.

Fig. 6 shows the maximum velocity of the annular jet and axial jets directed towards and away from the rigid boundary at the null final Kelvin impulse state as a function of the stand-off parameter γ. A first qualitative comment is that the maximum velocity reached by the radial jet is strikingly high with values of up to 36 at $\gamma = 0.9$. The radial jet velocity becomes smaller when γ is increased so that at $\gamma = 5$ the maximum jet velocity is about 6.5. It is worth noting here that, for $\gamma = 0.9$, the maximum velocity of the annular jet is reached at the end of the collapse. With increasing γ, the maximum velocity of this jet is reached in an earlier stage of the collapse. On the other hand, each axial jet is characterized by a critical value of γ at which the maximum velocity of the jet attains the highest value. It was found that an increase with one order of magnitude of the strength parameter α results in an increase of the maximum velocity of the jets with a factor of 6. At these high values the assumption of liquid incompressibility adopted in the present model is no longer justified. However, these results do give an indication of the violence of the collapse and the resulting non-spherical bubble behaviour when the bubble oscillates near the null final Kelvin impulse state.

4. Discussion

4.1. Jetting behaviour near the null final Kelvin impulse state

The results presented in the previous section revealed a very complex dynamics of a pulsating, buoyant bubble near a rigid boundary near the null final Kelvin impulse state. This includes formation of both radial and axial jets directed towards the bubble centre. The basic question we wish to address here is, why the bubble has so many types of behaviour for the same value of the Kelvin impulse at the conclusion of the collapse? A qualitative answer can be formulated by studying the Kelvin impulse during the collapse phase of the bubble. Fig. 7 shows the variation with time of the Kelvin impulse during the first oscillation period of the bubble for different initial location of the bubble from the boundary. The starting point in explaining the mechanisms

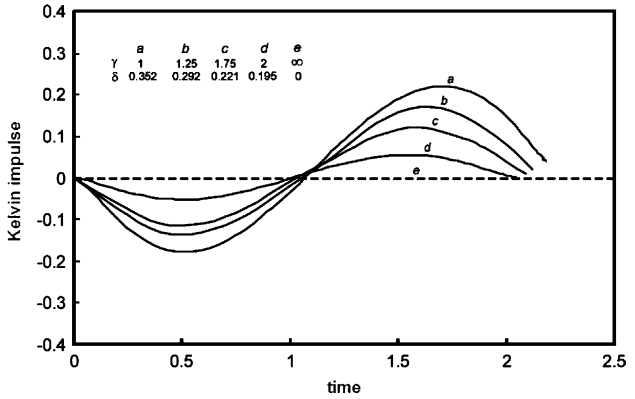

Fig. 7. Kelvin impulse during the oscillation period of a bubble at the null Kelvin impulse state.

governing the jetting behaviour is given by the observation that during the collapse phase of the bubble the Kelvin impulse is directed away from the boundary. Since the buoyancy force is proportional to the bubble volume and since the pressure-gradient force is strongly manifested only in the late collapse stages, the magnitude of the buoyancy force is larger over the entire collapse phase of the bubble.[1] Therefore, the radial flow is developed around the lower section of the bubble, in accord with the general principles of radial jet formation discussed above. Since the Kelvin impulse increases with decreasing γ, the radial flow is initiated closer to the lower pole of the bubble with lower γ. With increasing γ, the radial flow becomes more and more symmetric leading to the formation of a prolate shape of the bubble. According to Lauterborn (1982), jet formation can be explained by differently curved parts of the bubble surface, as the proportional relation between radius and collapse time (Rayleigh's formula) may be adopted for local radii as well. More highly curved parts of a bubble corresponding to a smaller bubble radius collapse faster than less curved parts leading to the formation of a liquid jet that threads the bubble. The top and bottom of the elongated bubble, i.e. the parts of the bubble with the highest curvature, collapses faster inducing the formation of two axial jets directed towards the bubble centre. The velocity of the upper axial jet is, however, larger than that of the lower axial jet to balance the increase of the Kelvin impulse due to the earlier formation of the lower jet. At very large γ-values, the velocity of the axial jets tends to become equal. Only in the limit $\gamma \to \infty$ and $\delta = 0$, the Kelvin impulse is zero over the whole oscillation period and the bubble keeps the spherical shape throughout its motion.

Unfortunately, despite the numerous experimental studies on the behaviour of underwater explosions near rigid boundaries (Menon and Lal, 1998; Kira et al., 1999; Rajendran and Narasimhan, 2001; and the references therein), no experimental data exist with which to make a direct comparison of our simulations. This fact is not surprising taking into account how small is the region centred around the null final Kelvin impulse state with the complex jetting behaviour.

[1] During the growth phase of the bubble the Kelvin impulse is directed towards the boundary because the bubble side nearest to the boundary moves into a region of higher relative impedance than the opposite side even though the velocities are similar. However, this feature has no consequence for jet formation.

More accurate experimental studies are needed before a confirmation of the present results becomes possible. Our results suggest, however, a violent collapse of the bubble in the neighbourhood of the null Kelvin impulse state. The most pronounced damage of the nearby boundary is likely to occur for γ-values smaller than one where the annular jet leads to bubble splitting and the formation of a high-speed axial jet directed towards the boundary. This jet is further accelerated by the shock waves emitted upon the collapse of the upper part of the bubble on the cavity closer to the boundary (see, for example, Brujan et al., 2001a). Besides this, the high pressure and temperature developed inside the collapsing bubble are also potential damage mechanisms of the nearby boundary.

4.2. A particular case: bubble motion between two parallel flat boundaries

A bubble oscillating between two parallel flat rigid boundaries is subjected to two opposite pressure-gradient forces. In this case, the null final Kelvin impulse state is obtained when the bubble is initiated at equal distance from the boundaries. It is here that the opposite pressure gradients acting on the bubble motion are of equal importance when summed over the bubble period and the Kelvin impulse is zero during both the growth and collapse phase of the bubble. Therefore, a symmetric radial flow is developed during bubble collapse. The experimental results of Chahine (1982) indicate that for small γ-values the radial flow determines the formation of an radial jet leading to bubble splitting and the formation of two axial jets of equal velocity directed towards and away from the boundary. Furthermore, the intensity of the radial flow becomes weaker and weaker with increasing the distance between the boundaries in agreement with the present result illustrated in Fig. 6. It is expected that for a sufficiently large distance between the boundaries the bubble achieves a prolate shape during collapse leading to the formation of two axial jets of equal velocity directed towards the bubble centre. Although no direct observation is available in the literature, the numerical calculations of Shima and Sato (1984) indicates that two opposite axial jets can be formed when a bubble with an initially prolate spheroidal shape collapses between two flat rigid boundaries. It should be noted here that an experimental evidence of this feature seems to be a real challenge since, as shown in Fig. 4, the axial jets are formed during the very late stage of the collapse when the bubble is near minimum volume.

5. Conclusions

The dynamics of a pulsating, buoyant bubble near a rigid boundary near the null final Kelvin impulse state is investigated numerically by using a boundary integral method. This case is particularly interesting because the opposing forces acting on the bubble, namely, the buoyancy force directed away from the boundary and the Bjerknes force directed towards the boundary, are of equal importance when summed over the bubble period at the end of the bubble collapse. The bubble dynamics shows a large variation in the jetting behaviour depending on the initial distance between bubble and boundary. The complex behaviour is attributed to a difference between the strength of the opposing forces during the collapse phase of the bubble.

The dominant feature of the bubble dynamics is the formation of a radial flow around the lower part of the bubble during collapse. The radial flow is a result of the oblate spheroidal shape of the

bubble at its maximum expansion, while the location of the jet-flow is a consequence of a relatively larger magnitude of the buoyancy force in the initial stage of the collapse. At larger γ-values, the bubble behaviour is characterized by the formation of two axial jets directed towards the bubble centre. This is a consequence of the prolate spheroidal shape of the collapsing cavity which, in turn, is caused by a more symmetric but weaker radial flow in the initial stage of the collapse.

The present results also demonstrate that the Kelvin impulse provides accurate predictions of the jetting behaviour even in the neighbourhood of the neutral collapse state of a bubble. The direction of the Kelvin impulse during the collapse phase of the bubble determines the position of the radial jet in the initial stage of the collapse while its magnitude indicates the location and the intensity of the radial jet. These are the essential factors in estimating the final fate of a bubble situated in opposing pressure gradients and near the neutral collapse state of the bubble. Away from this null-state, the final Kelvin impulse is an extremely valuable and accurate tool in predicting the migratory characteristics of the bubble and the direction of the axial jet developed during bubble collapse.

Acknowledgments

This study has been supported by EPSRC (Grant Nr. GR/N36868/01) by providing funds for a Visiting Fellowship for E.A. Brujan and an EPSRC Postgraduate Studentship for A. Pearson.

References

Benjamin, T.B., Ellis, A.T., 1966. The collapse of cavitation bubbles and the pressures thereby produced against solid boundaries. Philos. Trans. Royal Soc. London A 260, 221–240.

Best, J.P., 1991. The Dynamics of Underwater Explosions. PhD thesis, The University of Wollongong.

Best, J.P., Blake, J.R., 1992. Cavities, jets and toroidal bubbles. In: Proc. 3rd Int. Conf. Cavitation C453, Cambridge, pp. 17–22.

Best, J.P., Blake, J.R., 1994. An estimate of the Kelvin impulse of a transient cavity. J. Fluid Mech. 261, 75–93.

Best, J.P., Kucera, A., 1992. A numerical investigation of non-spherical rebounding bubbles. J. Fluid Mech. 245, 137–154.

Blake, J.R., 1988. The Kelvin impulse: Application to cavitation bubble dynamics. J. Aust. Math. Soc. B 30, 127–146.

Blake, J.R., Cerone, P., 1982. A note on the impulse due to a vapour bubble near a boundary. J. Aust. Math. Soc. B 23, 383–393.

Blake, J.R., Hooton, M.C., Robinson, P.B., Tong, R.P., 1997. Collapsing cavities, toroidal bubbles and jet impact. Philos. Trans. Royal Soc. London A 355, 537–550.

Blake, J.R., Taib, B.B., Doherty, G., 1986. Transient cavities near boundaries. Part 1. Rigid boundary. J. Fluid Mech. 170, 479–497.

Blake, J.R., Taib, B.B., Doherty, G., 1987. Transient cavities near boundaries. Part 2. Free surface. J. Fluid Mech. 181, 197–212.

Brujan, E.A., Nahen, K., Schmidt, P., Vogel, A., 2001a. Dynamics of laser-induced cavitation bubbles near an elastic boundary. J. Fluid Mech. 433, 251–281.

Brujan, E.A., Nahen, K., Schmidt, P., Vogel, A., 2001b. Dynamics of laser-induced cavitation bubbles near elastic boundaries: Influence of the elastic modulus. J. Fluid Mech. 433, 283–314.

Brujan, E.A., Keen, G.S., Vogel, A., Blake, J.R., 2002. The final stage of the collapse of a cavitation bubble close to a rigid boundary. Phys. Fluids 14, 85–92.

Chahine, G.L., 1982. Experimental and asymptotic study of nonspherical bubble collapse. Appl. Sci. Res. 38, 187–197.
Cole, R.H., 1948. Underwater Explosions. Princeton University Press.
Godwin, R.P., Chapyak, E.J., Noack, J., Vogel, A., 1999. Aspherical bubble dynamics and oscillation times. SPIE Proc. 3601, 225–237.
Kira, A., Fujita, M., Itoh, S., 1999. Underwater explosion of spherical explosives. J. Mater. Process. Technol. 85, 64–68.
Kornfeld, M., Suvorov, L., 1944. On the destructive action of cavitation. J. Appl. Phys. 15, 495–506.
Lauterborn, W., 1982. Cavitation bubble dynamics—new tools for an intricate problem. Appl. Sci. Res. 38, 165–178.
Menon, S., Lal, M., 1998. On the dynamics and instability of bubble formed during underwater explosions. Exp. Thermal Fluid Sci. 16, 305–321.
Pearson, A., Blake, J.R., Otto, S.R., 2004. Jets in bubbles. J. Eng. Math. 48, 391–412.
Plesset, M.S., Chapman, R.B., 1971. Collapse of an initially spherical vapour cavity in the neighbourhood of a solid boundary. J. Fluid Mech. 47, 283–290.
Prosperetti, A., Lezzi, A., 1986. Bubble dynamics in a compressible liquid. Part 1. First order theory. J. Fluid Mech. 168, 457–478.
Rajendran, R., Narasimhan, K., 2001. Linear elastic response of plane plates subjected to underwater explosions. Int. J. Impact Eng. 25, 493–506.
Rayleigh, Lord, 1917. On the pressure developed in a liquid during the collapse of a spherical cavity. Philos. Mag. 34, 94–98.
Robinson, P.B., Blake, J.R., 1994. Dynamics of cavitation bubble interactions. In: Blake, J.R., et al. (Eds.), Proc. IUTAM Symp. 'Bubble Dynamics and Interface Phenomena'. Kluwer, pp. 55–64.
Shima, A., Sato, Y., 1984. The collapse of a bubble between narrow parallel plates (The case where a bubble is attached to a solid wall). Rep. Inst. High Speed Mech., Tohoku Univ. 49, pp. 1–21.
Vogel, A., Lauterborn, W., Timm, R., 1989. Optical and acoustic investigations of the dynamics of laser-produced cavitation bubbles near a solid boundary. J. Fluid Mech. 206, 299–338.